OXFORD

ORIGINAL ARTICLE

Stimulation of S1PR$_5$ with A-971432, a selective agonist, preserves blood–brain barrier integrity and exerts therapeutic effect in an animal model of Huntington's disease

Alba Di Pardo[1], Salvatore Castaldo[1], Enrico Amico[1], Giuseppe Pepe[1], Federico Marracino[1], Luca Capocci[1], Alfredo Giovannelli[1], Michele Madonna[1], Jeroen van Bergeijk[2], Fabio Buttari[1], Elizabeth van der Kam[2] and Vittorio Maglione[1,*]

[1]IRCCS Neuromed, Localitá Camerelle, 86077, Pozzilli (IS), Italy and [2]AbbVie Deutschland GmbH & Co KG, Knollstrasse 50, 67061 Ludwigshafen, Germany

*To whom correspondence should be addressed at: Centre for Neurogenetics and Rare Diseases, IRCCS Neuromed, Pozzilli (IS) 86077, Italy. Tel: +39 0865915212; Fax: +39 0865927575; Email: vittorio.maglione@neuromed.it

Abstract

Huntington's disease (HD) is the most common neurodegenerative disorder for which no effective cure is yet available. Although several agents have been identified to provide benefits so far, the number of therapeutic options remains limited with only symptomatic treatment available. Over the past few years, we have demonstrated that sphingolipid-based approaches may open the door to new and more targeted treatments for the disease. In this study, we investigated the therapeutic potential of stimulating sphingosine-1-phosphate (S1P) receptor 5 by the new selective agonist A-971432 (provided by AbbVie) in R6/2 mice, a widely used HD animal model. Chronic administration of low-dose (0.1 mg/kg) A-971432 slowed down the progression of the disease and significantly prolonged lifespan in symptomatic R6/2 mice. Such beneficial effects were associated with activation of pro-survival pathways (BDNF, AKT and ERK) and with reduction of mutant huntingtin aggregation. A-971432 also protected blood–brain barrier (BBB) homeostasis in the same mice. Interestingly, when administered early in the disease, before any overt symptoms, A-971432 completely protected HD mice from the classic progressive motor deficit and preserved BBB integrity. Beside representing a promising strategy to take into consideration for the development of alternative therapeutic options for HD, selective stimulation of S1P receptor 5 may be also seen as an effective approach to target brain vasculature defects in the disease.

Introduction

Huntington's disease (HD) is the most common rare brain disorder characterized by progressive striatal and cortical degeneration and associated motor, cognitive and behavioural disturbances (1). The disease-causing mutation is a polyglutamine (polyQ) repeat expansion (>36 repeats) within huntingtin (Htt), a ubiquitous protein whose functions are not yet completely elucidated (2). Expansion of the polyQ stretch

endows mutant Htt (mHtt) with toxic properties, and results in the development of a broad array of cell dysfunctions in neuronal and non-neuronal cell populations (2–4).

A number of evidence demonstrates that an aberrant sphingolipid homeostasis represents an additional pathological event that may contribute to the pathogenesis of the disease (5–8). In this context, defective expression of the enzymes involved in the metabolism of sphingosine-1-phoshate (S1P) with the consequent reduction in its levels, may represent a critical pathological determinant in both experimental models and human patients (7,9–12).

S1P is a potent signaling bioactive sphingolipid that acts intracellularly as a second messenger and extracellularly in an autocrine and paracrine fashion by activating five known G protein-coupled receptors, $S1PR_{1-5}$, which are ubiquitously expressed throughout the body and in the central nervous system (CNS) (13). Among all, $S1PR_5$ is preferentially expressed in oligodendrocytes, where it may regulate lipid content and myelination (14) and in brain endothelial cells where it regulates blood–brain barrier (BBB) tight junctions (15), whose function is critical to paracellular transport and BBB permeability (16).

Impaired permeability of BBB has been described recently in HD in both human tissues and animal models even at early stages of the disease and it has been associated with reduced expression of Claudin-5 and Occludin (17,18), two key structural components of tight junction complex (16).

Defective brain vascular homeostasis may potentially be included as additional neuropathological hallmark of the disease and eventually identified as new a therapeutic target in the future.

Modulators of S1P receptors are currently used to treat different brain-related disorders (19), including Rett Syndrome and Amyotrophic Lateral Sclerosis (ALS) for which brain vasculature defects have also been described (20). Non-selective stimulation of S1P receptors by FTY720 (or Fingolimod), a FDA-approved drug for the treatment of multiple sclerosis, is neuroprotective and exerts disease-modifying effects also in multiple HD preclinical models (21,22).

In this study, we investigated the potential therapeutic benefits of a new selective brain penetrable $S1PR_5$ agonist, A-971432 (AbbVie) (23) in a HD animal model and explored its potential role in the maintenance of BBB integrity.

Treatment with 0.1 mg/kg (once daily) A-971432 blocked the progression of the disease and prolonged lifespan in symptomatic R6/2 mice. Interestingly, the compound delayed the onset of motor symptoms when administered early in the disease at the pre-symptomatic stage.

The beneficial effects on motor deficit were associated with activation of neuroprotective kinases AKT and ERK in the striatum, elevation in the levels of cortical brain-derived neurotrophic factor (BDNF) and with a significant amelioration of neuropathology. Beside reducing mHtt aggregation, A-971432 exerted protective action on BBB homeostasis and preserved its integrity.

Results

Chronic infusion of A-971432 prevents the worsening of motor deficit in symptomatic R6/2 mice

Stimulation of S1P receptors, by the non-selective modulator FTY720, has been previously reported to be beneficial in multiple HD pre-clinical models (21,22). To assess any therapeutic potential of more targeted stimulation, selective activation of $S1PR_5$ by A-971432 was investigated in symptomatic (7-week old) R6/2 mice and in age-matched wild-type (WT) littermates. Interestingly, chronic administration of A-971432 restored normal motor function in R6/2-treated mice within the first week of treatment, and preserved them from the gradual motor deficit, classically occurring during the disease, for the entire period of the treatment (Fig. 1A and B).

Interestingly, improved motor skills in R6/2 mice were associated with preserved body weight (Fig. 1C), whose loss is a classical hallmark of the disease progression (21,24), and significantly prolonged animal lifespan (Fig. 1D). No effects were observed in WT mice (Fig. 1A and D) and no evidence of adverse events were noted in none of the genotypes. In addition, pharmacokinetic analysis of mouse serum samples revealed an adequate exposure of A-971432 during the treatment comparable to previous studies (23) (Supplementary Material, Table S1).

Administration of A-971432 leads to the activation of neuroprotective pathways in the brain tissues from symptomatic R6/2 mice

Our previous studies indicate that stimulation of multiple S1P receptors exerts an overall neuroprotective action, evokes the activation of prosurvival AKT and ERK cell signalling pathways and increases the production of BDNF *in vivo* (21). Selective activation of $S1PR_5$ is also reported to sustain cell survival by promoting phosphorylation of AKT (14).

Here, we tested the possibility that A-971432, by selectively stimulating $S1PR_5$, might trigger the activation of similar prosurvival pathways in HD animals.

To this purpose, 1 h after i.p. administration of the compound, mice were sacrificed and brain tissues analyzed to assess phosphorylation rate of AKT and ERK as well as expression of BDNF. In line with our previous findings, administration of A-971432 leaded to increased phosphorylation of the two kinases (Fig. 2A and B) in the striatum of R6/2 mice and significantly incremented the levels of BDNF in the cortex (Fig. 2C).

Administration of A-971432 ameliorated neuropathology in symptomatic R6/2 mice

Next, with the aim of investigating any disease-modifying properties of the compound, neuropathological studies were carried out on brain tissues of R6/2 mice. First, the overall effect of A-971432 on the brain weight was evaluated. Chronic administration of A-971432 prevented the classic brain weight loss in R6/2 mice (Fig. 3A). Importantly, the compound had the benefits of lowering also mHtt toxic aggregates; its chronic administration was associated with reduced total number of cells containing EM48-immunoreactive mHtt aggregates as well as with decreased size of single aggregates in the striatum of treated R6/2 mice with respect to untreated controls (Fig. 3B–D). Reduction of mHtt aggregates after A-971432 treatment was also confirmed by immunoblotting analysis which showed a decrease of EM48-positive signal in the stacking part of the gel (Fig. 3E and Supplementary Material, Fig. S1).

Administration of A-971432-protected symptomatic R6/2 mice from progressive BBB dysfunctions

Impairment of BBB permeability and reduced expression of the tight junction proteins, Claudin-5 and Occludin, has been
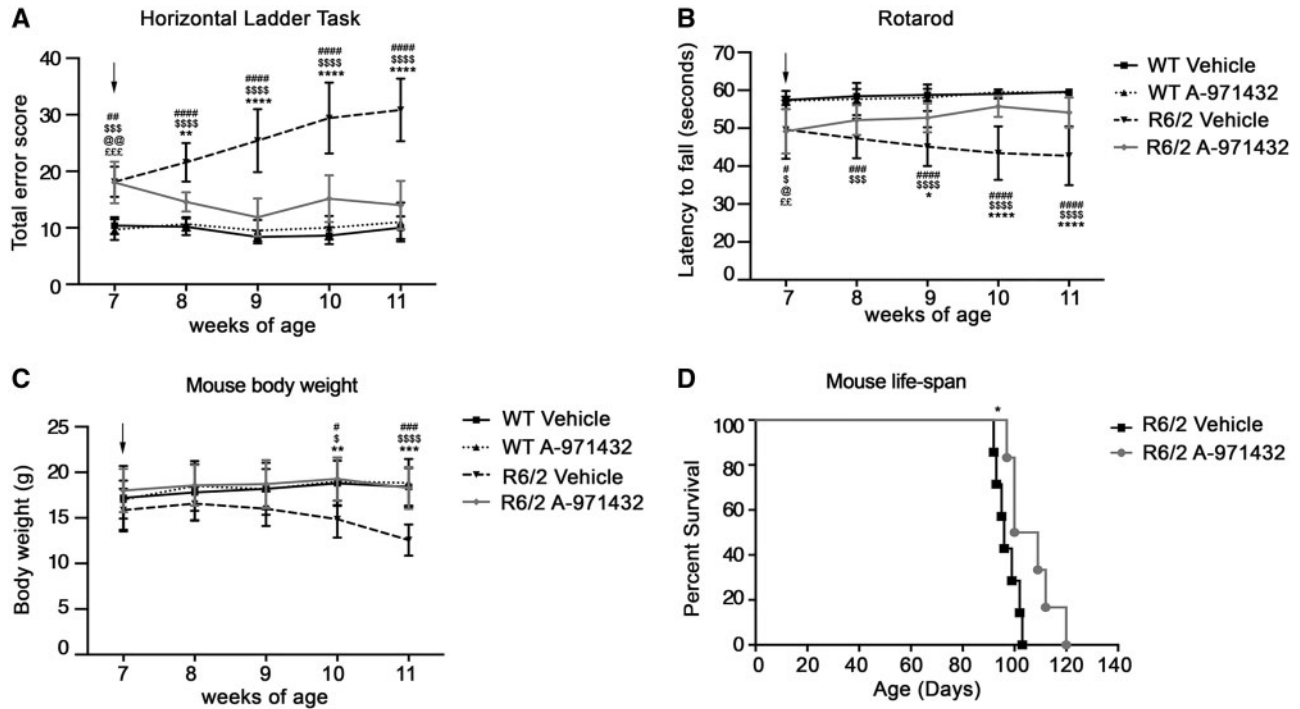
Figure 1. Administration of A-971432 preserves motor function in R6/2 mice. Motor performance assessed by horizontal ladder task (WT, $N = 6 + 6$; HD, $N = 8 + 8$) (**A**) and Rotarod (WT, $N = 6 + 6$; HD, $N = 8 + 9$) (**B**). Mouse body weight weekly measured during the entire period of the treatment (WT, $N = 6 + 6$; HD, $N = 8 + 8$) (**C**). Kaplan Maier curve of survival (HD, $N = 7 + 7$) (**D**). Arrows indicate when treatment started. Values are represented as mean ± SD. @, $P < 0.05$; @@, $P < 0.01$ (vehicle-treated WT vs. A971432-treated R6/2 mice). ££, $P < 0.01$; £££, $P < 0.001$ (A-971432-treated WT vs. A-971432-treated R6/2 mice). *, $P < 0.05$; **, $P < 0.01$; ***, $P < 0.001$; ****, $P < 0.0001$ (vehicle-treated R6/2 vs. A-971432-treated R6/2 mice). #, $P < 0.05$; ##, $P < 0.01$; ###, $P < 0.001$; ####, $P < 0.0001$ (vehicle-treated WT vs. vehicle-treated R6/2 mice). \$, $P < 0.05$; \$\$\$, $P < 0.001$; \$\$\$\$, $P < 0.0001$ (A-971432-treated WT vs. vehicle-treated R6/2 mice) (two-way ANOVA with Bonferroni post-test).
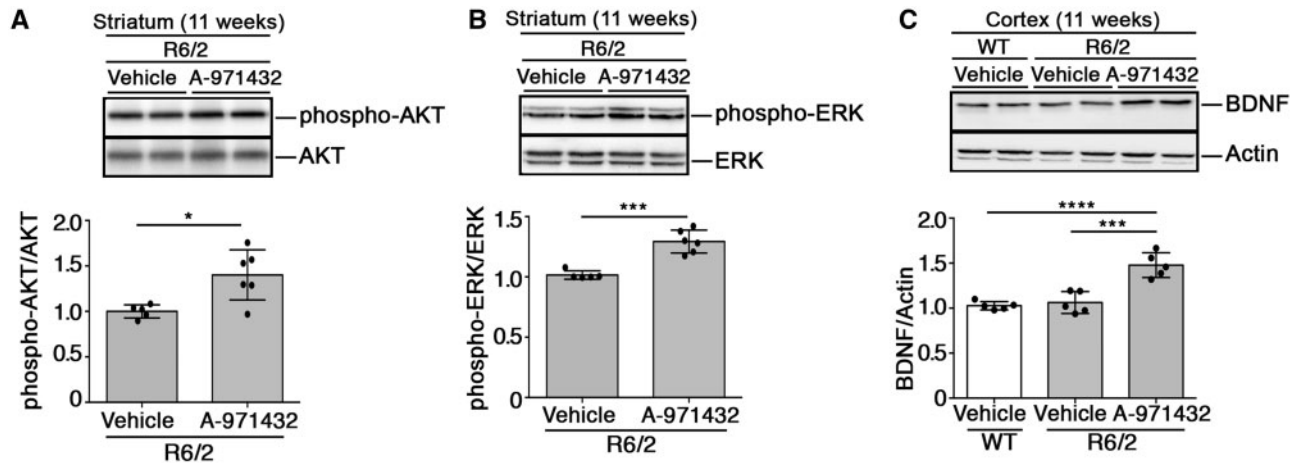

Figure 2. A-971432 promotes the activation of pro-survival pathways in brain tissues from R6/2 mice. Representative cropped western blottings and densitometric analysis of AKT (**A**) and ERK (**B**) phosphorylation levels in striatal tissues from vehicle- and A-971432-treated R6/2 mice at 11 weeks of age. Data are represented as mean ± SD. (HD, $N = 5 + 6$). *, $P < 0.05$; ***, $P < 0.001$ (unpaired *t*-test). Representative cropped western blottings and densitometric analysis of BDNF protein in cortical tissues from the same mice (**C**). Data are represented as mean ± SD. $N = 5$ for each group of mice. ***, $P < 0.001$; ****, $P < 0.0001$ (one-way ANOVA with Tukey post-test).

recently described in R6/2 mice ([17],[18]). BBB homeostasis is a quite complex condition and endothelial S1PR$_5$ in the brain has been reported to contribute to its integrity through regulation of tight junction protein levels ([15],[23]).

In the light of that, we explored the possibility that the selective targeting of S1PR$_5$, by A-971432, might regulate BBB permeability in symptomatic R6/2 mice, the only HD animal model where altered BBB is clearly described ([17],[18]). To this purpose,

at the end of the treatment, BBB leakage was assessed in symptomatic R6/2 mice and age-matched WT littermates, through the analysis of FITC-albumin extravasation into brain parenchymal as described previously ([18]).

Interestingly, in line with our expectation, chronic infusion of A-971432 attenuated the classic progressive BBB leakage and therefore the FITC-albumin extravasation in striatal parenchyma (Fig. 4A and B).
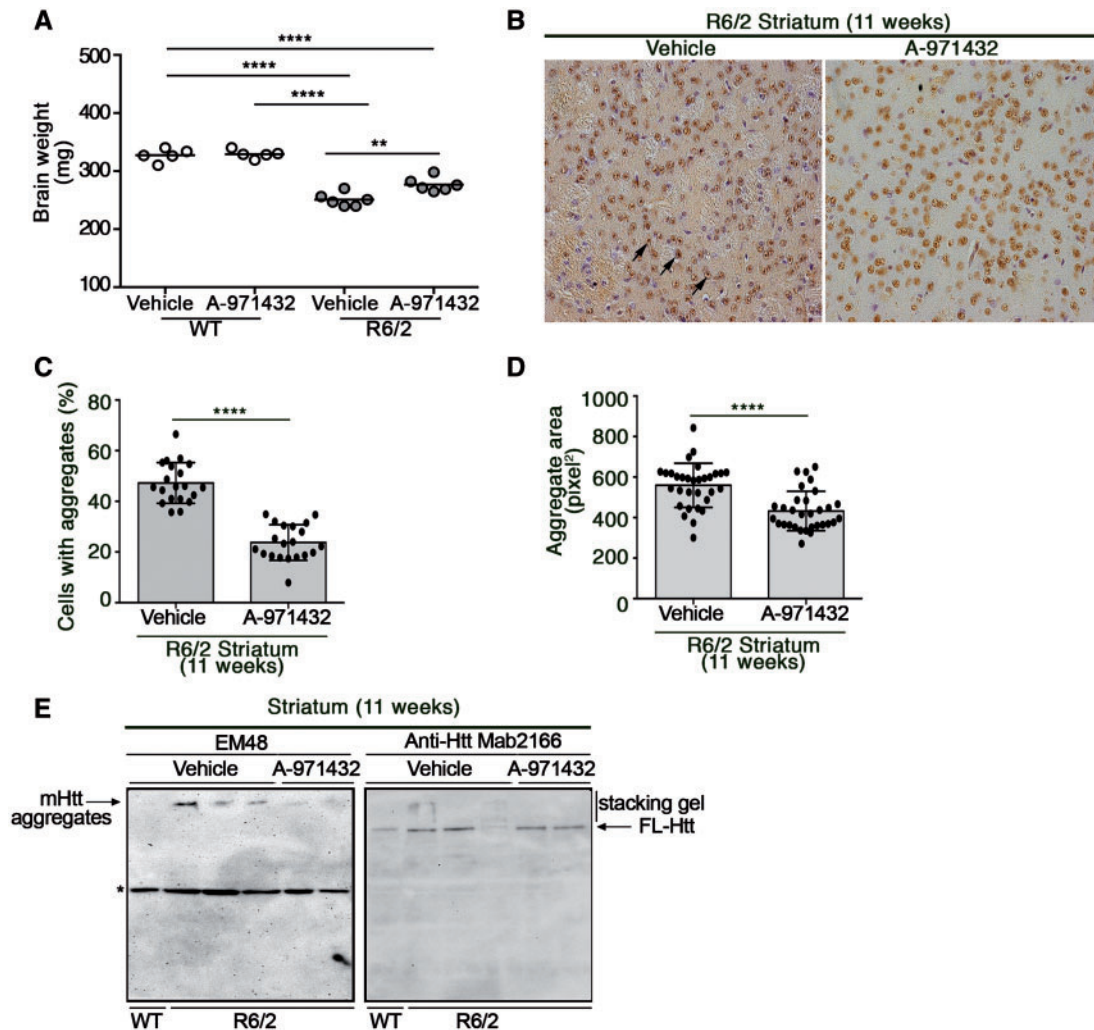
Figure 3. Administration of A-971432 ameliorates neuropathology in R6/2 mice. Mouse brain weight (WT, $N = 5 + 5$; HD, $N = 6 + 6$) (**A**). **, $P < 0.01$; ****, $P < 0.0001$ (one-way ANOVA with Tukey post-test). Representative micrograph (**B**), semi-quantitative analysis (**C**) of EM48-immunoreactive cells and aggregate area (**D**) in the striatum of vehicle- and A971432-treated R6/2 mice at 11 weeks of age. Arrows indicate mHtt aggregates. Scale bar in represents 100 μm. Values are represented as mean ± SD. WT, $N = 5 + 5$; HD, $N = 6 + 6$. ****, $P < 0.0001$ (unpaired *t*-test). (**E**) Immunoblotting showing EM48-positive mHtt aggregates and full-lenght Htt in striatal lysate from vehicle- and A-971432-treated R6/2 mice at 11 weeks of age. The asterisk (*) on the representative EM48 immunoblotting indicates an un-specific band recognized by the antibody.

Also, in order to further consolidate the association between tight junction stability and BBB leakage, levels of Occludin and Claudin-5 were examined in the treated mice. Immunoblotting analysis showed that chronic infusion of A-971432 significantly prevented the characteristic decrease in the expression of both proteins (Fig. 4C). The effect of the compound on tight junction proteins was also confirmed in WT mice (Supplementary Material, Fig. S2).

Early infusion of A-971432 preserved BBB integrity and delayed the onset of motor symptoms in R6/2 mice

We have recently demonstrated that first signs of BBB impairment become evident early in the disease in R6/2 mice, even before overt motor symptoms appear (18). Here, we explored the possibility that stimulation of S1PR5 might contribute to clarify any potential link between impairment of BBB integrity and disease onset. Thus, the ability of A-971432 to influence the occurrence of disease symptoms and to impact on BBB homeostasis

was explored in mice that received the compound starting from the pre-symptomatic (4-week old) stage of the disease (Figs 5 and 6). After 2 weeks of treatment, at the age of 6 weeks, when motor deficit is classically fully detectable in R6/2 mice (Fig. 5), A-971432 preserved normal motor function in treated mice with respect to untreated controls. Interestingly, treatment prevented the FITC-albumin extravasation, normally associated with this stage of the disease (18) (Fig. 6A and B). From biochemical point of view, maintained homeostasis of BBB after A-971432 was associated with normal levels of Occludin protein (Fig. 6C), but reduced levels of Claudin-5 (Fig. 6D).

Early administration of A-971432 suppresses aggregation of mHtt in the CNS blood vessels

Evidence shows accumulation of mHtt aggregates in brain vasculature of symptomatic R6/2 mice and human HD post mortem brains (17) and, the resulting compromise of the cerebral vasculature is suggestive of BBB damage in the disease (17). Here,
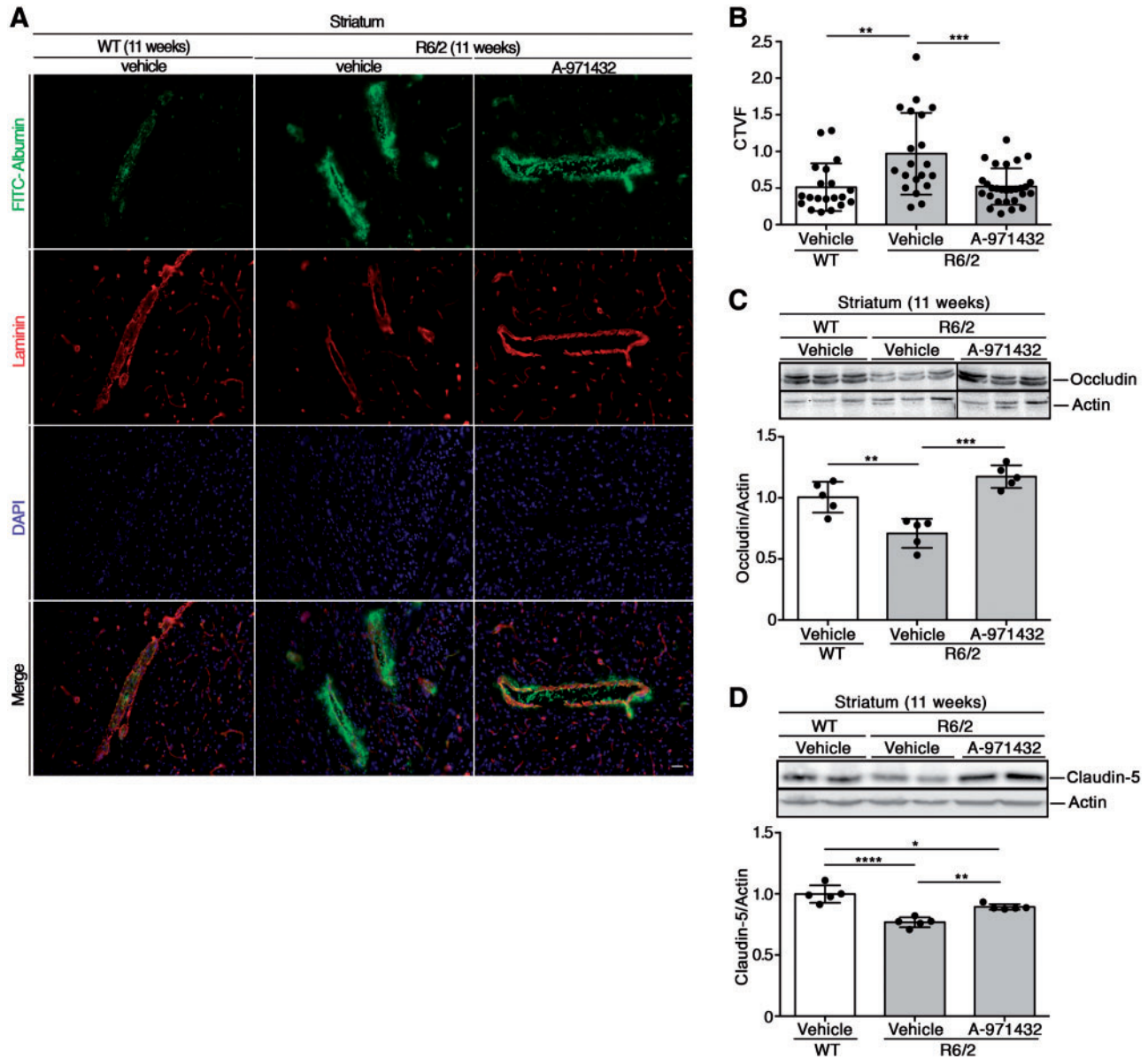
Figure 4. Administration of A-971432 attenuates striatal BBB defects in symptomatic R6/2 mice. Representative fluorescence micrographs (**A**) and semi-quantitative analysis (**B**) of FITC-albumin extravasation (bright green fluorescence) normalized on vessel marker laminin (red) in striatum of vehicle- and A-971432-treated R6/2 mice at 11 weeks of age and in age-matched WT controls. N = 5 for each group of mice. **, $P < 0.01$; ***, $P < 0.001$ (one-way ANOVA with Tukey post-test). CTVF, corrected total vessel fluorescence. Scale bar in the merge monograph represents 100 μm. Representative cropped western blottings and densitometric analysis of Occludin (**C**) and Claudin-5 (**D**) proteins in striatal tissues from the same mice. In each immunoblotting, all samples were run on the same gel. Non-adjacent samples were separated by a black line. N = 5 for each group of mice. *, $P < 0.05$; **, $P < 0.01$; ***, $P < 0.001$; ****, $P < 0.0001$ (one-way ANOVA with Tukey post-test).

with the aim to investigate whether there exists a possible link between BBB impairment and mHtt aggregation, we examined mutant protein organization in the wall of carotid arteries, normally considered a model for brain vasculature (25), from A-971432-treated and untreated R6/2 mice. Interestingly, maintained BBB homeostasis in A-971432-treated HD mice was associated with an attenuation of EM48-positive mHtt aggregate in carotid vessels as qualitatively detected by histological analysis (Fig. 7A). This result was quantitatively confirmed by immunoblottings that showed a significant decrease of SDS-insoluble mHtt aggregates as detected by EM48 antibody in the stacking part of the gels (Fig. 7B, C and D).

Discussion

Although numerous molecules have been screened for the development of new treatments for HD, the identification of novel and effective targets remains of great interest in HD. We and others have largely contributed to the recognition of S1P metabolism as new potential therapeutic target, and demonstrated that non-selective modulation of S1P receptors may represent an effective treatment in HD preclinical models (7,9,11,21,22,26).

In this study, we demonstrated for the first time, that A-971432, a new selective S1PR$_5$ agonist, is therapeutically effective in R6/2 mice, a widely used and well-characterized HD
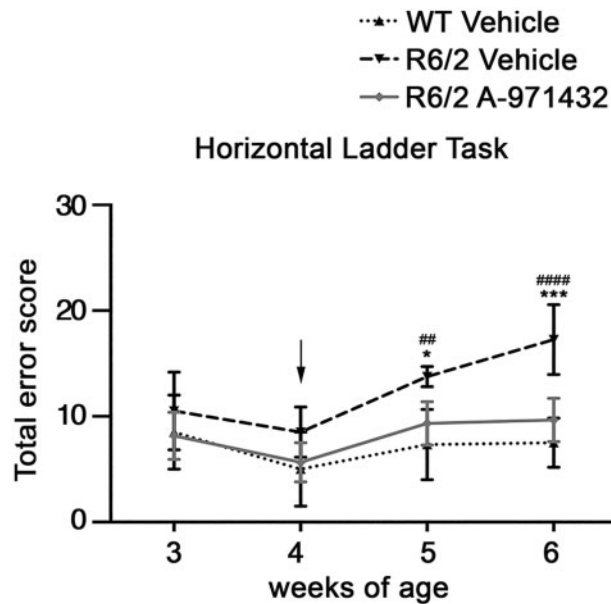
Figure 5. A-971432 delays the onset of motor deficit when administered in R6/2 mice starting from the pre-symptomatic stage. Mouse motor performance assessed by Horizontal Ladder Task (WT, $N = 4$; HD $= 5 + 6$). Arrows indicate when treatment started. $^{##}$, $P < 0.01$; $^{####}$, $P < 0.0001$ (vehicle- treated WT vs. vehicle-treated R6/2 mice); *, $P < 0.05$; ***, $P < 0.001$ (vehicle-treated R6/2 vs. A-971432-treated R6/2 mice) (two-way ANOVA with Bonferroni post-test).

animal model (27) which recapitulates many of the features of human pathology (28–32). Chronic administration of A-971432 protected symptomatic R6/2 mice from progressive motor deficit, normally associated with the disease course, and most importantly significantly delayed the onset of disease symptoms when administered in pre-symptomatic stage in the same mice.

Treatment with A-971432 exerted beneficial effect on physical well-being of the disease mouse model; it preserved normal body weight and significantly extended lifespan. From the mechanistic point of view, it is still unknown the exact underlying molecular mechanism, however, our findings revealed relevant molecular and neuropathological changes. Stimulation of S1PRs is generally associated with activation of cell signalling cascade (33). Coherently, A-971432 leaded to the activation/phosphorylation of pro-survival kinases AKT and ERK in brain tissues from HD mice. This is particularly important in the context of HD in which such kinase pathways are defective (34–36) and whose stimulation results neuroprotective (5,37–39). Also, A-971432-increased levels of the neurotrophin BDNF, whose signalling pathways have been reported to be aberrant in different neurodegenerative disorders (40,41), including HD (42), and whose restoration and/or enhanced bioavailability is widely described to provide major support for striatal neurons (43) also in R6/2 mice (44,45).

The molecular mechanisms by which A-971432 exerts beneficial effects in HD remain to be further elucidated, however, our results are coherent with other findings showing a correlation between stimulation of S1P axis and activation of neuroprotective pathways in pre-clinical models of a number of brain disorders, including HD (21,46,47).

Increased production of BDNF after A-971432 may likely represent the driving mechanism of neuroprotection in our study. Hypothetically it can be either a direct result of S1PR5 stimulation or an independent intracellular response, possibly related to the activation of AKT and ERK pathways (41,48–50).

Preservation of normal motor function after A-971432 administration in R6/2 mice well correlated with signs of neuroprotection like prevented loss of brain weight and dramatic reduction of EM48-positive mHtt aggregates in the striatum. Although it is still debated whether aggregates are the toxic mHtt species (51), interventions aimed at reducing their levels are beneficial in different HD models (52).

A strong point of this study is the protective effect that A-971432 has on BBB *in vivo*. In particular, attenuation of BBB leakage, detectable through the FITC-albumin extravasation in the brain parenchyma, is found after treatment either if started at symptomatic or at pre-symptomatic stage of the disease.

From a molecular standpoint, this 'functional' result was associated with an increased expression of the tight junction proteins, Occludin and Claudin-5, that are directly involved in regulating the integrity and proper functioning of the BBB (53,54). Pharmacological elevation of both Claudin-5 and Occludin levels increases trans-endothelial electrical resistance and decreases endothelial permeability (55,56). Interestingly, A-971432 has been reported to serve also as increaser of electrical resistance in an *in vitro* model of BBB integrity (23).

The protective action that A-971432 exerts on the BBB is likely attributable, at least in part, to the ability of the compound to maintain the normal function of tight junction by regulating the levels of key proteins like Occludin and Claudin-5. The effect of A-971432 administration on protein levels indicates that the compound is able to either restore normal protein setting in the tight junction organization or to partially prevent the characteristic reduction the proteins Occludin and Claudin-5 classically meet during the disease course (18).

The link between S1PR5 activation and change in the levels of tight junction protein is still under investigation in HD, however, *in vitro* available evidence demonstrates that the down regulation of the receptor leads to a reduction of Claudin-5 expression (15). Whether this is directly dependent on S1PR5 or secondary to downstream activated pathways is not clear yet, however, recent studies demonstrated that BDNF per se may modulate expression of both Occludin and Claudin-5 proteins in intestinal barrier (57,58).

Albeit A-971432 administered at the pre-symptomatic stage, failed to preserve levels of Claudin 5, R6/2 mice remained protected from BBB leakage. Although not clear yet, these finding suggest that the protective effect of A-971432 on BBB homeostasis may likely contemplate the involvement of a plethora of events ranging from functional to structural changes.

Indeed, beside other effects, A-971432 reduced the formation of mHtt aggregates in carotid arteries, which, albeit do not represent the classical brain vessels, may likely mirror brain vasculature response to the treatment.

How mHtt aggregates affect brain vascular system is not clear yet and further studies are certainly needed, however, evidence indicates that mHtt may affect endothelial architecture or interfere with transcytosis and para-cellular transport (17).

mHtt aggregates have been detected inside multiple components of the neurovascular unit like endothelial cells and pericytes (17) for which, S1P receptors, including S1PR5, contribute to proper functioning (15,59). In light of that, it is conceivable that reduction of mHtt aggregates, in vascular unit, may ameliorate vascular function and ultimately contribute to the BBB homeostasis.

To our best knowledge, this is the first and only evidence demonstrating that stimulation of S1PRs is critical for the structural and functional preservation of BBB in HD, whose impairment is becoming increasingly implicated in the pathogenesis
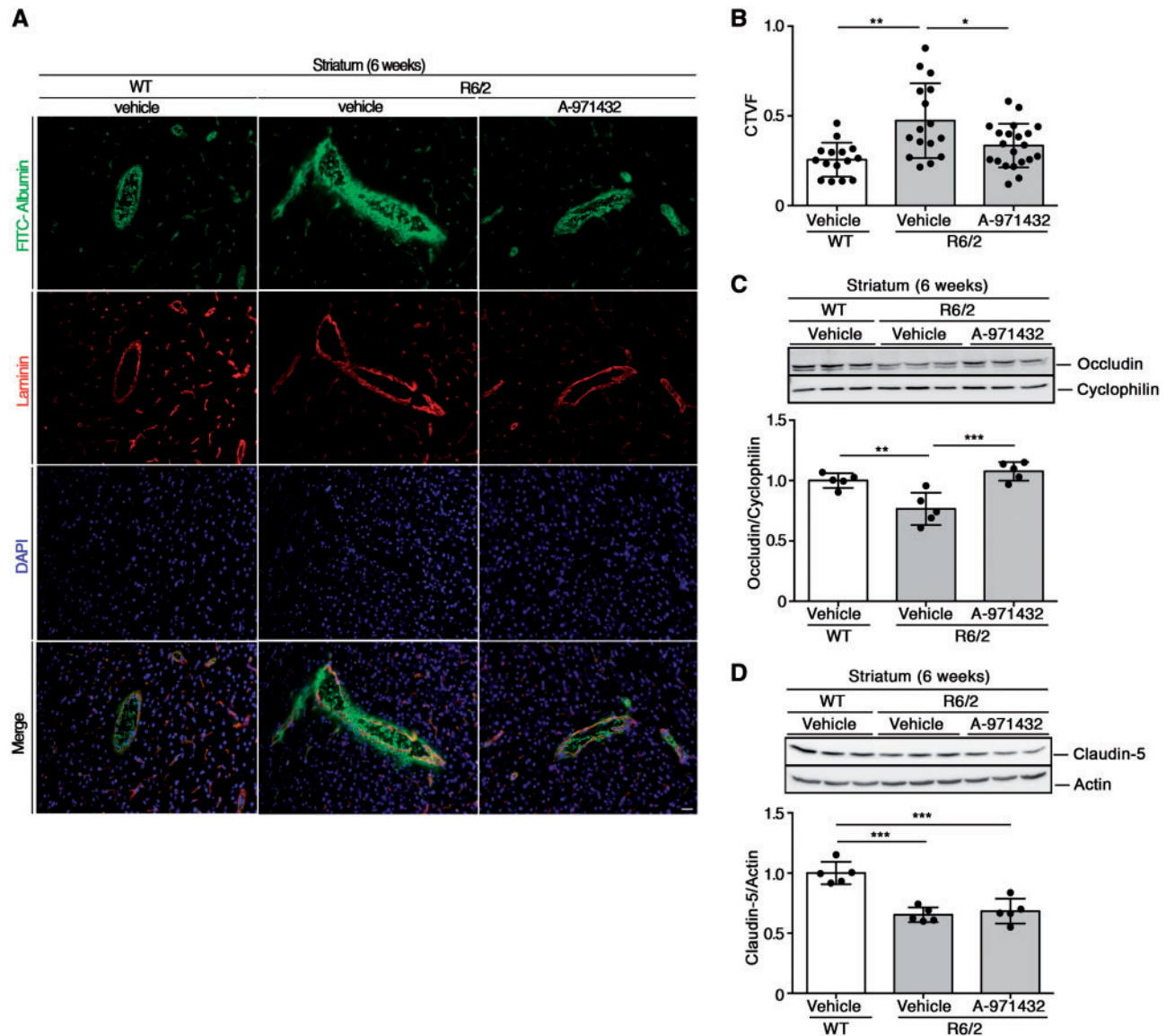
Figure 6. A-971432 prevents BBB defects when administered in R6/2 mice starting from the pre-symptomatic stage. Representative fluorescence micrographs (**A**) and semi-quantitative analysis (**B**) of FITC-Albumin extravasation (bright green fluorescence) normalized on vessel marker laminin (red) in striatum of vehicle- and A-971432-treated R6/2 mice at 6 weeks of age and age-matched WT controls. WT, $N = 4$; HD $= 5 + 6$. *, $P < 0.05$; **, $P < 0.01$ (one-way ANOVA with Tukey post-test). CTVF, corrected total vessel fluorescence. Scale bar in the merge monograph represents 100 µm. Representative cropped western blottings and densitometric analysis of Occludin (**C**) and Claudin-5 (**D**) proteins in striatal tissues from vehicle- and A-971432-treated mice at 6 weeks of age. $N = 5$ for each group of mice. **, $P < 0.01$; ***, $P < 0.001$ (one-way ANOVA with Tukey post-test).

of the disease. The significance of the interplay between defect of BBB and HD pathology still remains to be fully understood, however, our findings support the idea that compromised BBB seems to be strongly associated to first signs of the disease.

Recent evidence demonstrates that induction of neurovascular breakdown at pre-symptomatic stages of the disease in an animal model of ALS significantly accelerates motor symptoms and shortened mouse lifespan (20). Further studies are strongly warranted to establish any interdependency between these two events in HD.

Our findings are supported by current evidence sustaining a significant role for S1P signalling as a key determinant of BBB permeability and brain homeostasis and hence as a potential pathogenic player or therapeutic target in diseases characterized by both BBB dysfunction and neurodegeneration (60).

In this context, the therapeutic action of the S1PR5 stimulation by A-971432, in HD mice may represent a valuable 'druggable' target to develop more targeted and effective therapeutic approaches for the treatment of poorly explored aspects associated to the disease. Furthermore, the protective action that the compound exerts on the brain neuropathology indicates that A-971432 may serve also as a disease-modifying molecule with a great therapeutic potential. What makes A-971432 a very attractive compound is that stimulation of S1PR5 may have more limited immune suppressive and side effects as compared with drugs that either activate other S1P receptors (61,62) or have additional targets, as reported for FTY720, which may antagonize cannabinoid receptors (63), already reported to be down-regulated in HD (64).
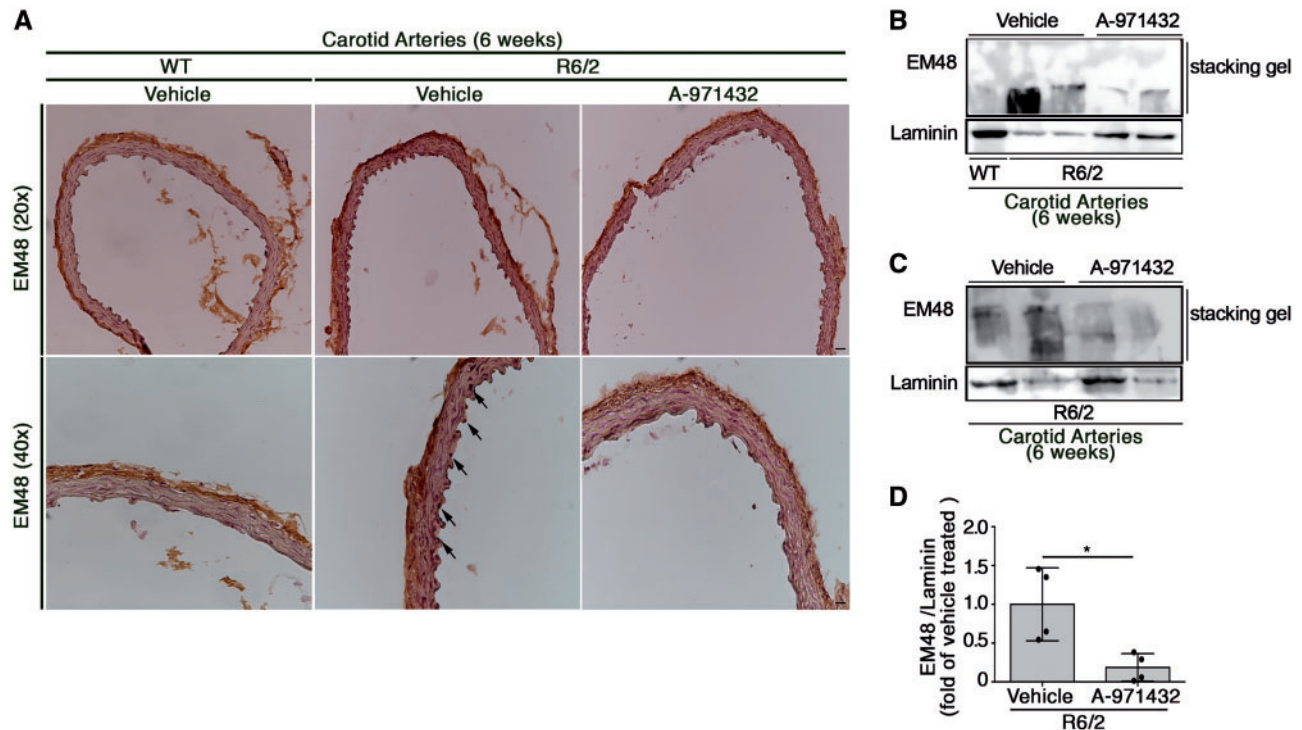
Figure 7. Administration of A-971432 reduces mHtt aggregation in carotid arteries from R6/2 mice. Representative micrographs (**A**), cropped immunoblottings (**B, C**) and densitometric analysis (**D**) of EM48-positive mHtt aggregates in carotid arteries from vehicle-treated WT mice and vehicle- and A-971432-treated R6/2 mice at 6 weeks of age. N = 4 for each group of R6/2 mice. *, P<0.05 (unpaired t-test). Scale bar represents 100 μm. Laminin was used as loading control.

A possible limitation of the study is the choice of only one animal model. However, R6/2 HD mice reflect, more than other pre-clinical models (65,66), the BBB abnormalities characterizing human HD pathology (17,18) and, therefore, they represent the best model available at moment for studying such structural defect and for eventually developing potential therapies.

Although our data need to be complemented by further studies, the present findings might contribute to figure out whether and how specific BBB drug targets can be approached in the future.

Our work may suggest important implications for disease pathogenesis and may help in formulating several new therapeutic strategies in humans. Such strategies may be designed either to directly target brain vascular structural abnormalities (i.e. tight junction proteins and/or other BBB components) or to develop sphingolipid-based approaches. In this context, A-971432 may represent a suitable drug for future clinical testing in HD.

Collectively, our findings demonstrate a potential correlation between BBB defects and the onset of motor deficits in HD and provide the first evidence that brain vasculature may represent a novel target for the development of novel therapeutic interventions for the disease.

Materials and Methods

Animal model

Breeding pairs of the R6/2 line of transgenic mice [strain name: B6CBA-tgN (HDexon1) 62Gpb/1J] with ~160 ± 10 (CAG) repeat expansions were purchased from the Jackson Laboratories. Male R6/2 mice were crossed with female B6CBA WT mice for colony maintenance. All procedures on animals were approved by the IRCCS Neuromed Animal Care Review Board and by

the 'Istituto Superiore di Sanità' (permit number: 1163/2015-PR) and were conducted according to EU Directive 2010/63/EU for animal experiments.

In vivo experiments were carried out in both R6/2 mice and WT littermates, starting from 3 or 7 weeks of age. To ensure homogeneity of experimental cohorts, mice from the same F generation were assigned to experimental groups, such that age and weight were matched. In total, 50 female R6/2 transgenic mice and 40 female WT littermates were used in this study. In order to reduce the number of animals used for this study, where possible, multiple biochemical analyses, evaluation and record of motor function were conducted on the same group of mice.

All animals used for biochemical and histological experiments were euthanized at fixed time points. Mice used for lifespan analysis died naturally.

In-vivo drug administration

A-971432 was dissolved in DMSO, further diluted in saline (vehicle) and daily administered by intraperitoneal (i.p.) injection at dose of 0.1 mg/kg of body weight starting either at 4 of age or 7 weeks of age as described previously (23). Control mice (WT and R6/2) were daily injected with the same volume of vehicle containing DMSO.

Motor behavior tests

Motor performance was assessed by Horizontal Ladder Task and Rotarod tests as described previously (21,67). All tests took place during the light phase of the light–dark cycle and mice

were tested before and after the initiation of the treatment at the indicated time points.

Brain lysate preparation

In order to clearly detect transient protein post-translation modification, like phosphorylation, mice were sacrificed within 1 h from the last treatment by cervical dislocation and brains were removed from the skull, weighed and bisected. Brains were immediately snap-frozen in liquid N_2 and pulverized in a mortar with a pestle. Pulverized tissue was then homogenized in lysis buffer containing 20 mm Tris, pH 7.4, 1% Nonidet P-40, 1 mm EDTA, 20 mm NaF, 2 mm Na_3VO_4 and protease inhibitor mixture (Santa Cruz, Cat. N. sc-29131), sonicated with 2×10 s pulses and then centrifuged for 10 min at 10 000g. Protein concentration was determined by Bradford method.

Immunoblottings

Proteins (40 μg) were resolved on 10% SDS-PAGE and immunoblotted with the following antibodies: anti-phospho-AKT (1: 1000) (Immunological Sciences Cat. N. AB-10521), anti-AKT (1: 1000) (Cell Signaling Cat. N. #2920), anti-phospho-ERK (1: 1000) (Immunological Sciences Cat. N. AB-10762), anti-ERK (1: 1000) (Cell Signaling, Cat. N. #4696), anti BDNF (1: 1000) (Santa Cruz, Cat. N. sc-546), anti-Occludin (Thermo Scientific, Cat. N. 710192) and anti-Claudin-5 (Abcam, Cat. N. ab15106). For protein normalization, anti-Actin (1: 5000) (Sigma Aldrich, Cat. N. A5441) was used. Immunoblots were then exposed to specific HRP-conjugated antibodies (Santa Cruz, Cat. N. sc-2004 and sc-2005). Protein bands were visualized by ECL Plus (GE Healthcare) and quantitated with Quantity One software (Bio-Rad Laboratories).

Analysis of striatal mHtt aggregates

WT and R6/2 mice were sacrificed by cervical dislocation. Brains were removed and trimmed by removing the olfactory bulbs and spinal cord. The remaining brain was processed and embedded in paraffin wax and 10 μm coronal sections were cut on an RM 2245 microtome (Leica Microsystems). Five mice/group ($n = 5$) were used and four coronal sections spread over the anterior-posterior extent of the brain (200–300 μm inter-section distance) were scanned. For each coronal section, a total number of 5 fields at 63× magnification were analyzed. Immunostaining for mHtt aggregates was carried out by using EM48 antibody (1: 200) (Millipore, Cat. N. 5374) as described previously (21). The average number of mHtt aggregate-containing cells per brain section was quantified by ImageJ software. For the immunoblotting analyses, cell lysate (40 μg) was resolved on 10% SDS-PAGE, entire gel, including the stacking portion, was transblotted over-night a 250 mV in 0.05% SDS and 16% methanol-containing transfer buffer (67). Membrane was blocked in 5% non-fat dry milk TBST for 1 h and successively immunoblotted with EM48 and/or anti Htt Mab2166 (Millipore) antibodies (both 1: 1000). A monoclonal anti-mouse HRP-conjugated antibody (Santa Cruz, Cat. N. sc-2005) was used as secondary antibody. Protein bands were visualized by ECL Plus (GE Healthcare).

Evaluation of blood–brain barrier permeability

BBB integrity was evaluated using FITC-Albumin (10 mg/ml in PBS at 10 ml/kg) (Sigma, Cat. N. A9771–100 MG) combined with Laminin (1: 1000) (Novus Biological, Cat N. NB300–144) immunostaining as described recently (18). A goat anti-rabbit CY3-conjugate (Millipore, Cat. N. AP132) was used as secondary antibody.

Fluorescence intensity for each single channel was analyzed by ImageJ software. Total fluorescent signal intensity of the FITC-albumin was normalized by the total CY3-Laminin fluorescent intensity per each image and reported as 'corrected total vessel fluorescence' (CTVF) as described (18,68,69).

Analysis of mHtt aggregates in carotid arteries

Mouse vessels were processed and embedded in paraffin wax and 10 μm coronal sections were cut on an RM 2245 microtome (Leica Microsystems). Immunostaining for mHtt aggregates was carried out by using EM48 antibody (1: 200) as reported above.

In the immunoblotting experiments, mouse carotid arteries were snap-frozen in liquid N_2 and pulverized in a mortar with a pestle. Pulverized tissue was then homogenized in 50 μl of lysis buffer containing 20 mm Tris, pH 7.4, 1% Nonidet P-40, 1 mm EDTA, 20 mm NaF, 2 mm Na_3VO_4 and protease inhibitor mixture (Santa Cruz, Cat. N. sc-29131), sonicated with 2×10 s pulses and then centrifuged for 10 min at 10 000g. Total protein lysate was then resolved on SDS-PAGE. Stacking gel portion was removed from the separating gel and transblotted over-night a 250 mV in 0.05% SDS and 16% methanol-containing transfer buffer. Membrane was blocked in 5% non-fat dry milk TBST for 1 h and successively immunoblotted with EM48 antibody (1: 500) and anti-Laminin antibody (1: 1000) (Novus Biological, Cat N. NB300–144). HRP-conjugated monoclonal and polyclonal antibodies (Santa Cruz, Cat. N. sc-2005 and sc-2004, respectively) were used as secondary antibodies. Protein bands were visualized by ECL Plus (GE Healthcare). Ponceau red staining was used as loading control.

Statistics

Two-way ANOVA followed by Bonferroni post-test was used to compare treatment groups with the Horizontal Ladder Task and Rotarod tests as well as for mouse body weight analysis. Log-rank test was used to analyze mouse survival. Two-tailed unpaired t-test and one-way ANOVA were used in all other experiments as indicated. All data were expressed as mean ± SD or as mean ± S.E.M. as indicated.

Supplementary Material

Supplementary Material is available at *HMG* online.

References

1. Walker, F.O. (2007) Huntington's disease. *Semin. Neurol.*, **27**, 143–150.

2. Zuccato, C., Valenza, M. and Cattaneo, E. (2010) Molecular mechanisms and potential therapeutical targets in Huntington's disease. *Physiol. Rev.*, **90**, 905–981.

3. Maglione, V., Cannella, M., Gradini, R., Cislaghi, G. and Squitieri, F. (2006) Huntingtin fragmentation and increased caspase 3, 8 and 9 activities in lymphoblasts with heterozygous and homozygous Huntington's disease mutation. *Mech. Ageing Dev.*, **127**, 213–216.

4. Maglione, V., Cannella, M., Martino, T., De Blasi, A., Frati, L. and Squitieri, F. (2006) The platelet maximum number of A2A-receptor binding sites (Bmax) linearly correlates with age at onset and CAG repeat expansion in Huntington's disease patients with predominant chorea. *Neurosci. Lett.*, **393**, 27–30.

5. Maglione, V., Marchi, P., Di Pardo, A., Lingrell, S., Horkey, M., Tidmarsh, E. and Sipione, S. (2010) Impaired ganglioside metabolism in Huntington's disease and neuroprotective role of GM1. *J. Neurosci.*, **30**, 4072–4080.

6. Di Pardo, A., Amico, E. and Maglione, V. (2016) Impaired levels of gangliosides in the corpus callosum of Huntington disease animal models. *Front. Neurosci.*, **10**, 457.

7. Di Pardo, A., Amico, E., Basit, A., Armirotti, A., Joshi, P., Neely, D.M., Vuono, R., Castaldo, S., Digilio, A.F., Scalabrì, F. *et al.* (2017) Defective sphingosine-1-phosphate metabolism is a druggable target in Huntington's disease. *Sci. Rep.*, **7**, 5280.

8. Skene, D.J., Middleton, B., Fraser, C.K., Pennings, J.L., Kuchel, T.R., Rudiger, S.R., Bawden, C.S. and Morton, A.J. (2017) Metabolic profiling of presymptomatic Huntington's disease sheep reveals novel biomarkers. *Sci. Rep.*, **7**, 43030.

9. Moruno Manchon, J.F., Uzor, N.E., Dabaghian, Y., Furr-Stimming, E.E., Finkbeiner, S. and Tsvetkov, A.S. (2015) Cytoplasmic sphingosine-1-phosphate pathway modulates neuronal autophagy. *Sci. Rep.*, **5**, 15213.

10. Pirhaji, L., Milani, P., Leidl, M., Curran, T., Avila-Pacheco, J., Clish, C.B., White, F.M., Saghatelian, A. and Fraenkel, E. (2016) Revealing disease-associated pathways by network integration of untargeted metabolomics. *Nat. Methods*, **13**, 770–776.

11. Pirhaji, L., Milani, P., Dalin, S., Wassie, B.T., Dunn, D.E., Fenster, R.J., Avila-Pacheco, J., Greengard, P., Clish, C.B., Heiman, M. *et al.* (2017) Identifying therapeutic targets by combining transcriptional data with ordinal clinical measurements. *Nat. Commun.*, **8**, 623.

12. Di Pardo, A., Basit, A., Armirotti, A., Amico, E., Castaldo, S., Pepe, G., Marracino, F., Buttari, F., Digilio, A.F. and Maglione, V. (2017) De novo synthesis of sphingolipids is defective in experimental models of Huntington's disease. *Front. Neurosci.*, **11**, 698.

13. Dev, K.K., Mullershausen, F., Mattes, H., Kuhn, R.R., Bilbe, G., Hoyer, D. and Mir, A. (2008) Brain sphingosine-1-phosphate receptors: implication for FTY720 in the treatment of multiple sclerosis. *Pharmacol. Ther.*, **117**, 77–93.

14. Jaillard, C., Harrison, S., Stankoff, B., Aigrot, M.S., Calver, A.R., Duddy, G., Walsh, F.S., Pangalos, M.N., Arimura, N., Kaibuchi, K. *et al.* (2005) Edg8/S1P5: an oligodendroglial receptor with dual function on process retraction and cell survival. *J. Neurosci.*, **25**, 1459–1469.

15. van Doorn, R., Lopes Pinheiro, M.A., Kooij, G., Lakeman, K., van het Hof, B., van der Pol, S.M., Geerts, D., van Horssen, J., van der Valk, P., van der Kam, E. *et al.* (2012) Sphingosine 1-phosphate receptor 5 mediates the immune quiescence of the human brain endothelial barrier. *J. Neuroinflam.*, **9**, 133.

16. Liu, W.Y., Wang, Z.B., Zhang, L.C., Wei, X. and Li, L. (2012) Tight junction in blood-brain barrier: an overview of structure, regulation, and regulator substances. *CNS Neurosci. Ther.*, **18**, 609–615.

17. Drouin-Ouellet, J., Sawiak, S.J., Cisbani, G., Lagace, M., Kuan, W.L., Saint-Pierre, M., Dury, R.J., Alata, W., St-Amour, I., Mason, S.L. *et al.* (2015) Cerebrovascular and blood-brain barrier impairments in Huntington's disease: potential implications for its pathophysiology. *Ann. Neurol.*, **78**, 160–177.

18. Di Pardo, A., Amico, E., Scalabri, F., Pepe, G., Castaldo, S., Elifani, F., Capocci, L., De Sanctis, C., Comerci, L., Pompeo, F. *et al.* (2017) Impairment of blood-brain barrier is an early event in R6/2 mouse model of Huntington Disease. *Sci. Rep.*, **7**, 41316.

19. O'Sullivan, S. and Dev, K.K. (2017) Sphingosine-1-phosphate receptor therapies: advances in clinical trials for CNS-related diseases. *Neuropharmacology*, **113**, 597–607.

20. Winkler, E.A., Sengillo, J.D., Sagare, A.P., Zhao, Z., Ma, Q., Zuniga, E., Wang, Y., Zhong, Z., Sullivan, J.S., Griffin, J.H. *et al.* (2014) Blood-spinal cord barrier disruption contributes to early motor-neuron degeneration in ALS-model mice. *Proc. Natl. Acad. Sci. U.S.A.*, **111**, E1035–E1042.

21. Di Pardo, A., Amico, E., Favellato, M., Castrataro, R., Fucile, S., Squitieri, F. and Maglione, V. (2014) FTY720 (fingolimod) is a neuroprotective and disease-modifying agent in cellular and mouse models of Huntington disease. *Hum. Mol. Genet.*, **23**, 2251–2265.

22. Miguez, A., Garcia-Diaz Barriga, G., Brito, V., Straccia, M., Giralt, A., Gines, S., Canals, J.M. and Alberch, J. (2015) Fingolimod (FTY720) enhances hippocampal synaptic plasticity and memory in Huntington's disease by preventing p75NTR up-regulation and astrocyte-mediated inflammation. *Hum. Mol. Genet.*, **24**, 4958–4970.

23. Hobson, A.D., Harris, C.M., van der Kam, E.L., Turner, S.C., Abibi, A., Aguirre, A.L., Bousquet, P., Kebede, T., Konopacki, D.B., Gintant, G. *et al.* (2015) Discovery of A-971432, an orally bioavailable selective sphingosine-1-phosphate receptor 5 (s1p5) agonist for the potential treatment of neurodegenerative disorders. *J. Med. Chem.*, **58**, 9154–9170.

24. van der Burg, J.M.M., Gardiner, S.L., Ludolph, A.C., Landwehrmeyer, G.B., Roos, R.A.C. and Aziz, N.A. (2017) Body weight is a robust predictor of clinical progression in Huntington disease. *Ann. Neurol.*, **82**, 479–483.

25. DeLeo, M.J., 3rd, Gounis, M.J., Hong, B., Ford, J.C., Wakhloo, A.K. and Bogdanov, A.A. Jr. (2009) Carotid artery brain aneurysm model: in vivo molecular enzyme-specific MR imaging of active inflammation in a pilot study. *Radiology*, **252**, 696–703.

26. Moruno-Manchon, J.F., Uzor, N.E., Blasco-Conesa, M.P., Mannuru, S., Putluri, N., Furr-Stimming, E.E. and Tsvetkov, A.S. (2017) Inhibiting sphingosine kinase 2 mitigates mutant Huntingtin-induced neurodegeneration in neuron models of Huntington disease. *Hum. Mol. Genet.*, **26**, 1305–1317.

27. Chang, R., Liu, X., Li, S. and Li, X.J. (2015) Transgenic animal models for study of the pathogenesis of Huntington's disease and therapy. *Drug Des. Devel. Ther.*, **9**, 2179–2188.

28. Neueder, A., Landles, C., Ghosh, R., Howland, D., Myers, R.H., Faull, R.L.M., Tabrizi, S.J. and Bates, G.P. (2017) The pathogenic exon 1 HTT protein is produced by incomplete splicing in Huntington's disease patients. *Sci. Rep.*, **7**, 1307.

29. Mangiarini, L., Sathasivam, K., Seller, M., Cozens, B., Harper, A., Hetherington, C., Lawton, M., Trottier, Y., Lehrach, H., Davies, S.W. *et al.* (1996) Exon 1 of the HD gene with an

expanded CAG repeat is sufficient to cause a progressive neurological phenotype in transgenic mice. *Cell*, **87**, 493–506.

30. Davies, S.W. and Scherzinger, E. (1997) Nuclear inclusions in Huntington's disease. *Trends Cell Biol.*, **7**, 422.

31. Carter, R.J., Lione, L.A., Humby, T., Mangiarini, L., Mahal, A., Bates, G.P., Dunnett, S.B. and Morton, A.J. (1999) Characterization of progressive motor deficits in mice transgenic for the human Huntington's disease mutation. *J. Neurosci.*, **19**, 3248–3257.

32. Vonsattel, J.P. (2007) Huntington disease models and human neuropathology: similarities and differences. *Acta Neuropathol.*, **115**, 55–69.

33. Brinkmann, V. (2007) Sphingosine 1-phosphate receptors in health and disease: mechanistic insights from gene deletion studies and reverse pharmacology. *Pharmacol. Ther.*, **115**, 84–105.

34. Apostol, B.L., Illes, K., Pallos, J., Bodai, L., Wu, J., Strand, A., Schweitzer, E.S., Olson, J.M., Kazantsev, A., Marsh, J.L. *et al.* (2006) Mutant huntingtin alters MAPK signaling pathways in PC12 and striatal cells: ERK1/2 protects against mutant huntingtin-associated toxicity. *Hum. Mol. Genet.*, **15**, 273–285.

35. Colin, E., Regulier, E., Perrin, V., Durr, A., Brice, A., Aebischer, P., Deglon, N., Humbert, S. and Saudou, F. (2005) Akt is altered in an animal model of Huntington's disease and in patients. *Eur. J. Neurosci.*, **21**, 1478–1488.

36. Varma, H., Yamamoto, A., Sarantos, M.R., Hughes, R.E. and Stockwell, B.R. (2010) Mutant huntingtin alters cell fate in response to microtubule depolymerization via the GEF-H1-RhoA-ERK pathway. *J. Biol. Chem.*, **285**, 37445–37457.

37. Humbert, S., Bryson, E.A., Cordelieres, F.P., Connors, N.C., Datta, S.R., Finkbeiner, S., Greenberg, M.E. and Saudou, F. (2002) The IGF-1/Akt pathway is neuroprotective in Huntington's disease and involves Huntingtin phosphorylation by Akt. *Dev. Cell*, **2**, 831–837.

38. Bodai, L. and Marsh, J.L. (2012) A novel target for Huntington's disease: eRK at the crossroads of signaling. The ERK signaling pathway is implicated in Huntington's disease and its upregulation ameliorates pathology. *Bioessays*, **34**, 142–148.

39. Sarantos, M.R., Papanikolaou, T., Ellerby, L.M. and Hughes, R.E. (2012) Pizotifen activates ERK and provides neuroprotection in vitro and in vivo in models of Huntington's disease. *J. Huntingtons Dis.*, **1**, 195–210.

40. Budni, J., Bellettini-Santos, T., Mina, F., Garcez, M.L. and Zugno, A.I. (2015) The involvement of BDNF, NGF and GDNF in aging and Alzheimer's disease. *Aging Dis.*, **6**, 331–341.

41. Bathina, S. and Das, U.N. (2015) Brain-derived neurotrophic factor and its clinical implications. *Arch. Med. Sci.*, **11**, 1164–1178.

42. Zuccato, C. and Cattaneo, E. (2009) Brain-derived neurotrophic factor in neurodegenerative diseases. *Nat. Rev. Neurol.*, **5**, 311–322.

43. Binder, D.K. and Scharfman, H.E. (2004) Brain-derived neurotrophic factor. *Growth Factors*, **22**, 123–131.

44. Giampa, C., Montagna, E., Dato, C., Melone, M.A., Bernardi, G. and Fusco, F.R. (2013) Systemic delivery of recombinant brain derived neurotrophic factor (BDNF) in the R6/2 mouse model of Huntington's disease. *PLoS One*, **8**, e64037.

45. Giralt, A., Carreton, O., Lao-Peregrin, C., Martin, E.D. and Alberch, J. (2011) Conditional BDNF release under pathological conditions improves Huntington's disease pathology by delaying neuronal dysfunction. *Mol. Neurodegener.*, **6**, 71.

46. Deogracias, R., Yazdani, M., Dekkers, M.P., Guy, J., Ionescu, M.C., Vogt, K.E. and Barde, Y.A. (2012) Fingolimod, a sphingosine-1 phosphate receptor modulator, increases BDNF levels and improves symptoms of a mouse model of Rett syndrome. *Proc. Natl. Acad. Sci. U.S.A.*, **109**, 14230–14235.

47. Ren, M., Han, M., Wei, X., Guo, Y., Shi, H., Zhang, X., Perez, R.G. and Lou, H. (2017) FTY720 attenuates 6-OHDA-associated dopaminergic degeneration in cellular and mouse Parkinsonian models. *Neurochem. Res.*, **42**, 686–696.

48. Qiao, L.Y., Yu, S.J., Kay, J.C. and Xia, C.M. (2013) In vivo regulation of brain-derived neurotrophic factor in dorsal root ganglia is mediated by nerve growth factor-triggered Akt activation during cystitis. *PLoS One*, **8**, e81547.

49. Hisaoka-Nakashima, K., Kajitani, N., Kaneko, M., Shigetou, T., Kasai, M., Matsumoto, C., Yokoe, T., Azuma, H., Takebayashi, M., Morioka, N. *et al.* (2016) Amitriptyline induces brain-derived neurotrophic factor (BDNF) mRNA expression through ERK-dependent modulation of multiple BDNF mRNA variants in primary cultured rat cortical astrocytes and microglia. *Brain Res.*, **1634**, 57–67.

50. Johnson-Farley, N.N., Patel, K., Kim, D. and Cowen, D.S. (2007) Interaction of FGF-2 with IGF-1 and BDNF in stimulating Akt, ERK, and neuronal survival in hippocampal cultures. *Brain Res.*, **1154**, 40–49.

51. Arrasate, M., Mitra, S., Schweitzer, E.S., Segal, M.R. and Finkbeiner, S. (2004) Inclusion body formation reduces levels of mutant huntingtin and the risk of neuronal death. *Nature*, **431**, 805–810.

52. Sanchez, I., Mahlke, C. and Yuan, J. (2003) Pivotal role of oligomerization in expanded polyglutamine neurodegenerative disorders. *Nature*, **421**, 373–379.

53. Feldman, G.J., Mullin, J.M. and Ryan, M.P. (2005) Occludin: structure, function and regulation. *Adv. Drug Deliv. Rev.*, **57**, 883–917.

54. Piontek, J., Winkler, L., Wolburg, H., Muller, S.L., Zuleger, N., Piehl, C., Wiesner, B., Krause, G. and Blasig, I.E. (2008) Formation of tight junction: determinants of homophilic interaction between classic claudins. *Faseb J.*, **22**, 146–158.

55. Honda, M., Nakagawa, S., Hayashi, K., Kitagawa, N., Tsutsumi, K., Nagata, I. and Niwa, M. (2006) Adrenomedullin improves the blood-brain barrier function through the expression of claudin-5. *Cell Mol. Neurobiol.*, **26**, 109–118.

56. McCarthy, K.M., Skare, I.B., Stankewich, M.C., Furuse, M., Tsukita, S., Rogers, R.A., Lynch, R.D. and Schneeberger, E.E. (1996) Occludin is a functional component of the tight junction. *J. Cell Sci.*, **109 (Pt 9)**, 2287–2298.

57. Yu, Y.B., Zhao, D.Y., Qi, Q.Q., Long, X., Li, X., Chen, F.X. and Zuo, X.L. (2017) BDNF modulates intestinal barrier integrity through regulating the expression of tight junction proteins. *Neurogastroenterol. Motil.*, **29**, e12967.

58. Zhao, D.Y., Zhang, W.X., Qi, Q.Q., Long, X., Li, X., Yu, Y.B. and Zuo, X.L. (2018) Brain-derived neurotrophic factor modulates intestinal barrier by inhibiting intestinal epithelial cells apoptosis in mice. *Physiol. Res.*, in press.

59. Li, Y., Lucas-Osma, A.M., Black, S., Bandet, M.V., Stephens, M.J., Vavrek, R., Sanelli, L., Fenrich, K.K., Di Narzo, A.F., Dracheva, S. *et al.* (2017) Pericytes impair capillary blood flow and motor function after chronic spinal cord injury. *Nat. Med.*, **23**, 733–741.

60. Prager, B., Spampinato, S.F. and Ransohoff, R.M. (2015) Sphingosine 1-phosphate signaling at the blood-brain barrier. *Trends Mol. Med.*, **21**, 354–363.

61. Park, S.J. and Im, D.S. (2017) Sphingosine 1-phosphate receptor modulators and drug discovery. *Biomol. Ther.*, **25**, 80–90.

62. Gonzalez-Cabrera, P.J., Brown, S., Studer, S.M. and Rosen, H. (2014) S1P signaling: new therapies and opportunities. *F1000Prime Rep.*, **6**, 109.

63. Paugh, S.W., Cassidy, M.P., He, H., Milstien, S., Sim-Selley, L.J., Spiegel, S. and Selley, D.E. (2006) Sphingosine and its analog, the immunosuppressant 2-amino-2-(2-[4-octylphenyl]ethyl)-1, 3-propanediol, interact with the CB1 cannabinoid receptor. *Mol. Pharmacol.*, **70**, 41–50.

64. Basavarajappa, B.S., Shivakumar, M., Joshi, V. and Subbanna, S. (2017) Endocannabinoid system in neurodegenerative disorders. *J. Neurochem.*, **142**, 624–648.

65. Mantovani, S., Gordon, R., Li, R., Christie, D.C., Kumar, V. and Woodruff, T.M. (2016) Motor deficits associated with Huntington's disease occur in the absence of striatal degeneration in BACHD transgenic mice. *Hum. Mol. Genet.*, **25**, 1780–1791.

66. Franciosi, S., Ryu, J.K., Shim, Y., Hill, A., Connolly, C., Hayden, M.R., McLarnon, J.G. and Leavitt, B.R. (2012) Age-dependent neurovascular abnormalities and altered microglial morphology in the YAC128 mouse model of Huntington disease. *Neurobiol. Dis.*, **45**, 438–449.

67. Di Pardo, A., Maglione, V., Alpaugh, M., Horkey, M., Atwal, R.S., Sassone, J., Ciammola, A., Steffan, J.S., Fouad, K., Truant, R. *et al.* (2012) Ganglioside GM1 induces phosphorylation of mutant huntingtin and restores normal motor behavior in Huntington disease mice. *Proc. Natl. Acad. Sci. U.S.A.*, **109**, 3528–3533.

68. McCloy, R.A., Rogers, S., Caldon, C.E., Lorca, T., Castro, A. and Burgess, A. (2014) Partial inhibition of Cdk1 in G 2 phase overrides the SAC and decouples mitotic events. *Cell Cycle*, **13**, 1400–1412.

69. Burgess, A., Vigneron, S., Brioudes, E., Labbe, J.C., Lorca, T. and Castro, A. (2010) Loss of human Greatwall results in G2 arrest and multiple mitotic defects due to deregulation of the cyclin B-Cdc2/PP2A balance. *Proc. Natl. Acad. Sci. U.S.A.*, **107**, 12564–12569.